Computers & Geosciences 92 (2016) 21–37

Contents lists available at ScienceDirect

Computers & Geosciences

journal homepage: www.elsevier.com/locate/cageo

Review article

Drainage networks and watersheds delineation derived from TIN-based digital elevation models

Henrique Rennó de Azeredo Freitas *, Corina da Costa Freitas, Sergio Rosim, João Ricardo de Freitas Oliveira

National Institute for Space Research, Image Processing Division, PO BOX 515, 12.227-010, São José dos Campos, SP, Brazil

ARTICLE INFO

Article history:
Received 23 April 2015
Received in revised form
24 December 2015
Accepted 4 April 2016
Available online 6 April 2016

Keywords:
Digital elevation models
Triangulated irregular networks
Flat areas
Pits
Drainage networks
Watersheds delineation

ABSTRACT

Triangulated Irregular Networks (TIN) efficiently define terrain models from which drainage networks and watersheds can be extracted with important applications in hydrology. In this work, the TIN model is represented by a constrained Delaunay triangulation obtained from contour lines and sampled points. Paths of steepest descent calculated from the TIN are connected by processing the triangles according to an associated priority, then forming a drainage graph structure proposed to generate drainage networks from accumulated flows. Major problems such as flat areas and pits that create inconsistencies in the terrain model and discontinuities in flows are removed with procedures that interpolate the elevation values of particular points on the TIN. Drainage networks are defined by arbitrary threshold values, and their associated watersheds and subwatersheds are then delineated. TIN results are qualitatively and quantitatively compared to an available reference drainage network, and also to regular grid results generated with the TerraHidro system. The drainage networks automatically obtained from the drainage graph highly agree to the main courses of water on the terrain, indicating that the TIN is an attractive alternative terrain model for hydrological purposes, and that the proposed drainage graph can be used for the automatic extraction of drainage networks that are consistent with real-world hydrological patterns.

© 2016 Elsevier Ltd. All rights reserved.

Contents

* Corresponding author.
E-mail addresses: henrique.renno@inpe.br (H.R.d.A. Freitas), corina@dpi.inpe.br (C.d.C. Freitas), sergio@dpi.inpe.br (S. Rosim), joao@dpi.inpe.br (J.R.d.F. Oliveira).

http://dx.doi.org/10.1016/j.cageo.2016.04.003
0098-3004/© 2016 Elsevier Ltd. All rights reserved.

1. Introduction

Terrain surfaces are generally represented by Digital Elevation Models (DEM) with relevant and useful applications in many areas of natural sciences. More specifically, hydrology applications commonly use terrain models to automate the generation of flow directions, drainage networks and watersheds that are essential elements in the understanding of hydrological processes. Usually, DEMs involve some distinct schemes: a rectangular grid of points; a set of points scattered over the surface and connected as a triangulation; or contour lines, normally presented in topographic maps (Jones et al., 1990).

The most simple and used DEM is the regular grid (Fowler and Little, 1979; Petrie and Kennie, 1987) that is widely available from many sources, such as the Shuttle Radar Topography Mission (SRTM) provided by the CGIAR-CSI (Jarvis et al., 2008) and the Global Land Survey Digital Elevation Model (GLSDEM) from the USGS (USGS, 2008). In a regular grid, elevation values are assigned to points or cells uniformly distributed over space as a two-dimensional matrix, thus depending on the grid resolution it may be well adjusted in regions with high variation in the elevation values although spatially redundant in regions where the elevation variation is low or non-existent.

Despite the extensive use of regular grids, terrain surfaces are not regular structures in nature, so their representation is not required to be regular. Besides the main advantage of a simple 2D structure, some drawbacks of regular grids as terrain models are: (a) if terrain surface points are obtained from land-surveying techniques, then each grid cell is assigned an interpolated elevation value, and much of the information from the original elevation data is lost in the interpolation process (Jones et al., 1990); (b) the storage of highly redundant data in regions of smooth terrain (Fowler and Little, 1979), thus presenting flat areas and making the extraction of drainage paths relatively difficult for any method, especially the ones based on local operations (O'Callaghan and Mark, 1984); (c) flow directions restricted to only eight different possibilities as defined from the D8 algorithm (Jenson and Domingue, 1988; O'Callaghan and Mark, 1984) that might generate unnatural drainage patterns; (d) higher computational and storage costs for more detailed spatial information in hydrological modeling, significantly limiting efficient distributed model calibration and real-time execution, so that large-scale applications usually produce average results with coarse model resolutions, implying in the distortion of the simulated hydrological dynamics (Ivanov et al., 2004). The extraction of drainage networks and watersheds from regular grids is extensively considered in several works (Abreu et al., 2012; Fowler and Little, 1979; Jenson and Domingue, 1988; O'Callaghan and Mark, 1984) with a wide range of applications in water resources.

Another type of DEM is the Triangulated Irregular Network (TIN) (Berg et al., 2008; Jones et al., 1990; Petrie and Kennie, 1987) that defines an efficient and flexible terrain model with multiple resolutions offered by the irregular domain (Ivanov et al., 2004). In a TIN, the density of information can vary from region to region, so more points are included where there is more variation in elevation whereas fewer points are necessary in regions of less variation, thus reducing computational and storage costs, and avoiding data redundancy. The terrain surface is modeled by several triangles generated from a set of points distributed over space according to some selected criteria, each point defined by a triple (x, y, z) with x and y being the coordinates on the horizontal plane, and z being the elevation. These points ideally constitute the main characteristics and features of the terrain, so that a TIN efficiently adapts to its irregularities and provides a more accurate representation of the original data (Jones et al., 1990) because the elevation of each point is not modified, and the triangles define linear planes where new points can be interpolated.

Moreover, if a TIN contains as many triangles as cells in a regular grid for some region, sampling and selection of very important points (VIP) from the grid allows the generation of a TIN terrain model without loss in detail of the spatial information of the topography, and with substantial savings in storage. The increasing availability of terrain models as regular grids make it desirable to devise methods for the selection of particular points from the grid that characterize surface-specific features such as ridges, hills, peaks, saddles, channels, valleys, and pits in order to be further triangulated.

Different approaches for VIP selection are: (a) local operations on each point, subtracting the point elevation from the elevation of its neighbors in either clockwise or counterclockwise sequences around the point, then classifying it as a particular surface feature from the pattern of positive and negative differences (Peucker and Douglas, 1975); (b) geometric operators of image processing for edges extraction to identify possible ridges or channels, both subsequently simplified by keeping only significant points, and iteratively refined with successive triangulations (Fowler and Little, 1979); (c) use of high-pass filters to calculate a significant degree of a point, change it according to its distance to the line formed by two neighboring points in four cases, and then compare to a histogram of significance distribution (Chen and Guevara, 1987).

Many distinct triangulations can be calculated from the same set of points, although it is necessary to obtain a triangulation that results in a good approximation for terrain modeling, given by the Delaunay triangulation (Berg et al., 2008; Bowyer, 1981; Cignoni et al., 1998; Fortune, 1987; Guibas et al., 1992; Jones et al., 1990; O'Rourke, 1998; Tsai, 1993; Watson, 1981) because it avoids the generation of skinny triangles. In this work, the points to be triangulated define contour lines and sampled points extracted from contour maps, and the Delaunay triangulation calculated from this set of points is likely to produce edges that cross the contour lines resulting in spurious terrain features, so intersections are removed with a further procedure that modifies edges of the triangulation considering each contour line as a restriction line that cannot be crossed, thus defining a constrained Delaunay triangulation (Zhu and Yan, 2010) that maintains the main characteristics and features of the terrain surface.

Additionally, major problems that also occur in terrain models are the existence of flat areas and pits. In a TIN, flat areas are formed by triangles with the three points or vertices of same elevation whereas pits are points where no neighboring point connected by a triangle edge is lower. These problems hinder the definition of flow directions, creating hydrological inconsistencies in the terrain model to be avoided. For this reason, flat areas are removed by an improved procedure modified from a previous work (Barbalic et al., 1999) that inserts new points into the triangulation with interpolated elevation values after defining paths of flat triangles (Freitas et al., 2013; Freitas, 2014). Similarly, the procedure for pit removal defines paths of points that start from the pit, and traverses triangles edges until reaching a lower point (Silveira and van Oostrum, 2007; Silveira, 2009), then the elevation of each point is re-interpolated.

The generation of more exact and sophisticated terrain models brings many possibilities of being used in computational systems known as GIS (Geographic Information System). Furthermore, hydrology-specific functionalities can be added in a GIS for the automatic extraction of flow directions, drainage networks and watersheds, although most GIS applications have limited capabilities in modeling flows on a TIN, so that this type of functionality is less developed for TINs than for regular grids. In general, TIN datasets used for terrain modeling raise challenges in the development of efficient algorithms to extract useful results because it usually involves complex tasks of computational geometry.

This work presents a new algorithm for the extraction of drainage networks from a TIN based on the gradient method (Jones et al., 1990) with flow directions defined by the gradient vectors of the triangles. The new algorithm traces drainage paths that strictly follow paths of steepest descent from the triangles ordered with the centroid's elevation as an associated priority, and then connects the paths to generate a drainage graph structure (Freitas, 2014). The proposed drainage graph is the main contribution of this work, and it allows to derive drainage networks and watersheds from accumulated flows.

2. TIN correction

2.1. Flat areas

Flat areas on terrain surfaces usually occur in regions of low slope such as landscapes of flood plains and prairies in contrast to regions with more significant changes in elevation that present higher slopes. Surfaces of lakes, sloughs or other water bodies may also characterize flat areas. Although these flat regions do not commonly have overland flows, the presence of flat areas in terrain models is considered an inconsistency because flow directions are not defined, so it prevents continuity of flows, and turns out to be a major problem in hydrological computations. For this reason, this work performs procedures to automatically remove flat areas in order to ensure that drainage paths are fully connected.

More specifically, flat areas on TINs occur at triangles with three vertices of same elevation, and since this work uses contour lines as input data, the resulting triangulation is likely to contain flat triangles because all the points of a contour line have the same elevation. In this work, flat areas are removed with the insertion of new points into the TIN, where each new point has an interpolated elevation. These points are considered as critical points placed at the middle of critical edges (Fig. 1) identified by two cases: (a) an edge connecting non-consecutive points on the same contour line; (b) an edge connecting points of different contour lines but of same elevation (Eastman, 2001).

After determining the critical edges, all the triangles with only one critical edge are selected, namely corner triangles, to be used as initial triangles for the definition of a path with the critical points where elevation values are interpolated (Barbalic et al., 1999). The path of triangles is defined by a depth-first search starting at a corner triangle, then traversing through adjacent triangles that share common critical edges, so that each unvisited triangle determines a new critical point for interpolation (Fig. 2).

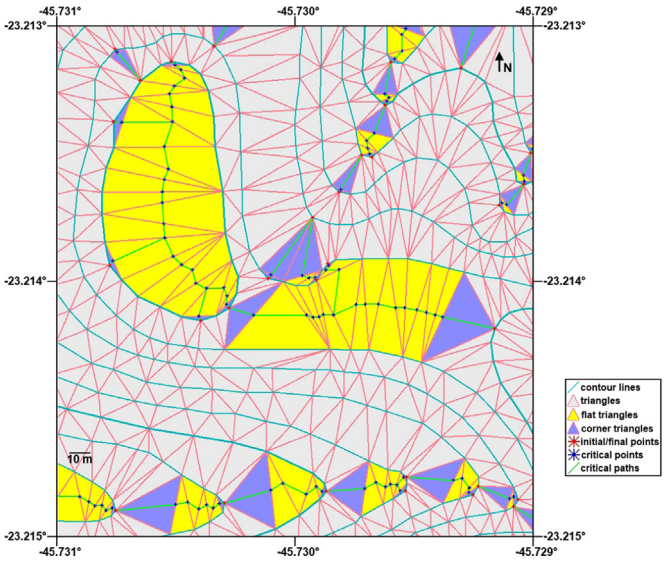

Fig. 2. Paths of triangles in flat areas are initiated at corner triangles defining critical points for interpolation between initial and final points.

The point that connects the two non-critical edges of the corner triangle is considered as the first point of the path, and the search terminates when another corner triangle with a point of different elevation is reached, considered then as the final point. Finally, the elevations of the critical points are linearly interpolated between the elevations of the initial and final points.

The linear interpolation of elevation values considers the lengths of the segments in a path as the distance from each critical point to the initial point (Eq. (1)) that results in a weight factor to interpolate the elevation of each critical point cp_m (Eq. (2)) (Freitas et al., 2013). The value $length_k$ represents the distance between the critical points indexed by k and $k-1$, where the points cp_0 and cp_n are the initial and final points, respectively, in a path with $n+1$ points. The value $dist_m$ is the distance from the critical point cp_m to the initial point and $dist_n$ is the distance between the initial and final points:

$$dist_m = \sum_{k=1}^{m} length_k \tag{1}$$

$$cp_m = \frac{dist_m}{dist_n}(cp_n - cp_0) + cp_0 \tag{2}$$

Branches found when traversing triangles with three critical edges are also processed after the assignment of interpolated

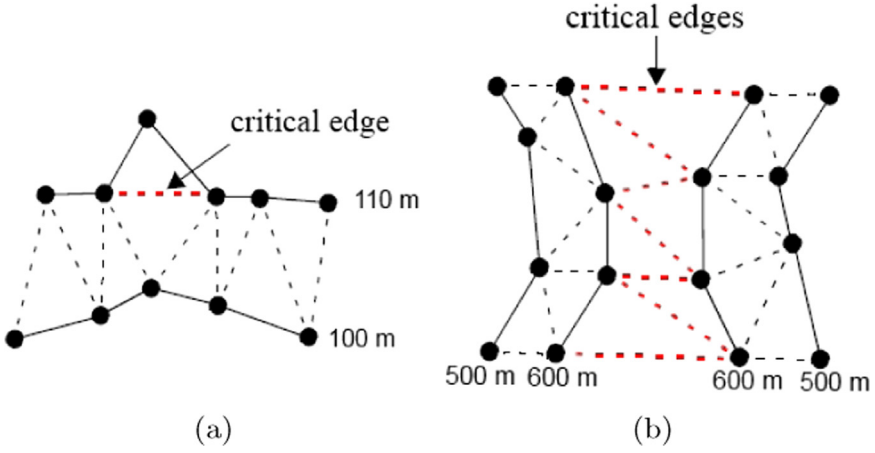

Fig. 1. Triangles (dashed lines) from contour lines (solid lines) with critical edges (red) (adapted from Eastman, 2001). (For interpretation of the references to color in this figure caption, the reader is referred to the web version of this paper.)

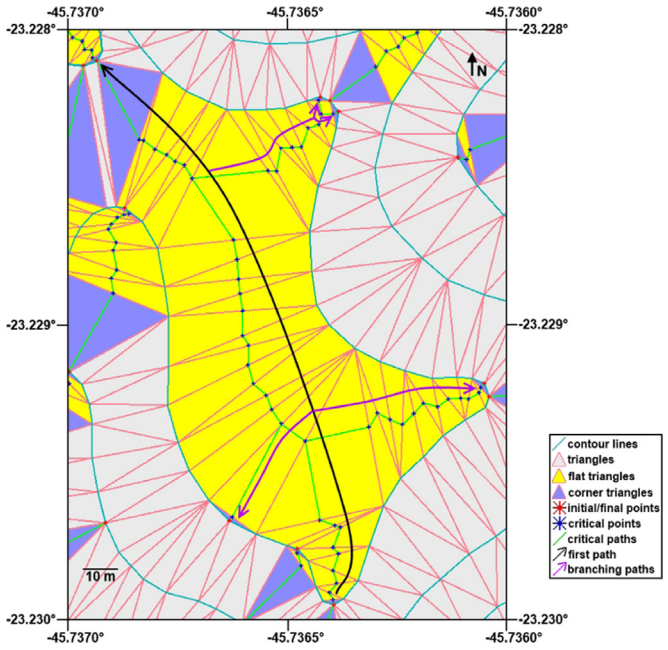

Fig. 3. Path with critical points to be first interpolated (black arrow) and branching paths with critical points to be interpolated next (purple arrows). (For interpretation of the references to color in this figure caption, the reader is referred to the web version of this paper.)

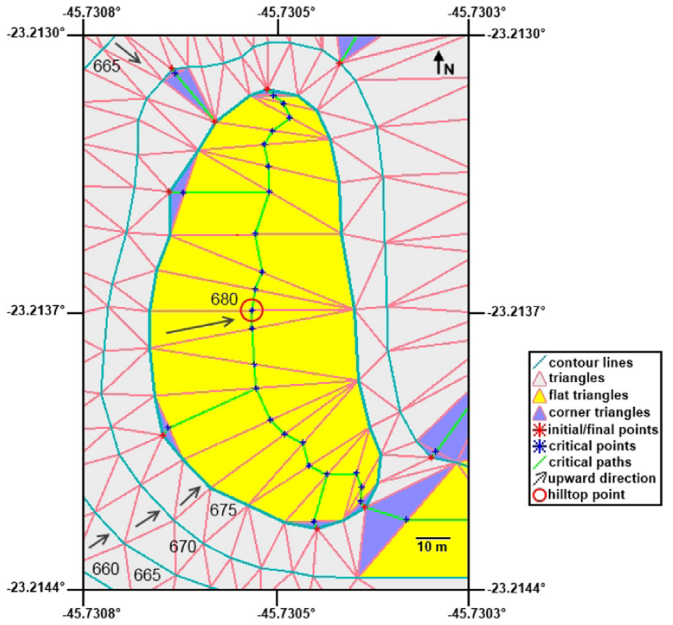

Fig. 4. Interpolation of critical points defines a hilltop. (For interpretation of the references to color in this figure, the reader is referred to the web version of this paper.)

elevations to each critical point of the first path. The search then repeats beginning at each branching triangle, although the initial points are chosen from the critical points of the branching triangles where elevations are already interpolated (Freitas et al., 2013). This procedure is performed until all the critical points are assigned interpolated elevations, and then inserted into the triangulation. Fig. 3 depicts branching paths of flat triangles defined in a flat area.

However, there are cases where the initial and final points in any path have the same elevation, and the interpolation of the critical points is not possible to be performed. These cases are: (a) the paths of triangles are inside a closed contour line that defines only flat triangles in its interior; (b) a path of triangles where the initial and final points have the same elevation, although of different elevation relative to the flat area elevation. The procedure described so far does not consider these cases, so a proposed simple solution defines an improvement that works in both cases.

In Fig. 4, the closed flat area is surrounded by a lower contour line, so one of the critical points is assigned an elevation higher than the flat area resulting in a hilltop, then defining the final point for interpolation. More precisely, the critical point located in the middle of the first path (red circle) is assigned the flat area elevation incremented by the elevation variation between contour lines.

Fig. 5 illustrates the case where the neighboring contour lines of each flat triangle are lower but the corner triangles have points of higher elevations relative to the flat area elevation. Similarly, the half-way critical point of the first path (red circle) is assigned a new elevation, although in this case calculated as the mean value between the elevation of the flat area and the elevation of either the initial or the final point, then resulting in a saddle point.

In order to outline the description of how the algorithm removes flat areas, a simplified pseudo-code including the functions that define paths of triangles with critical points where elevations are interpolated is appended at the end of the document.

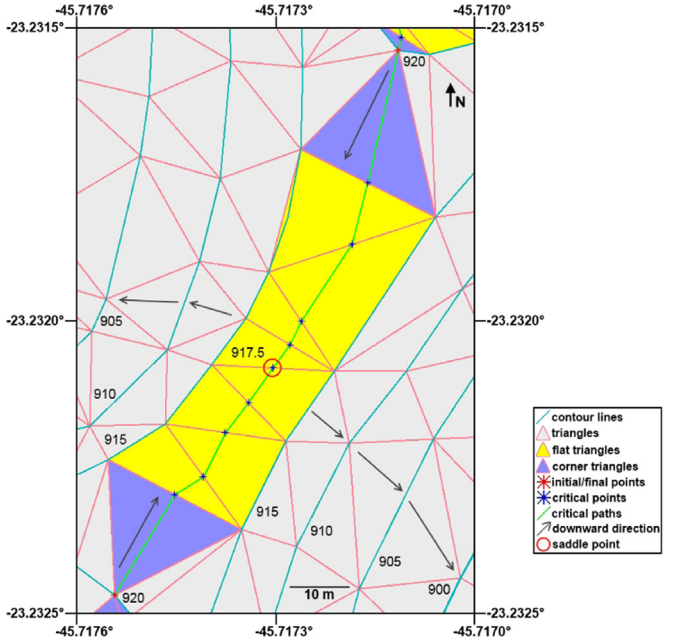

Fig. 5. Mean value between contour lines is assigned to a particular critical point. (For interpretation of the references to color in this figure, the reader is referred to the web version of this paper.)

2.2. Pits

Pits are generally considered as inaccurate data on DEMs because most of the depressions in terrains are likely to be spurious features (Silveira and van Oostrum, 2007), although water bodies on the surface may also characterize pits. Moreover, hydrological applications that use terrain models are often affected by the presence of pits because flows passing through these points do not follow any direction, thus hindering flow routing and determining discontinuities to be avoided. In a TIN, pits occur at points where no neighboring point connected by a triangle edge has lower elevation.

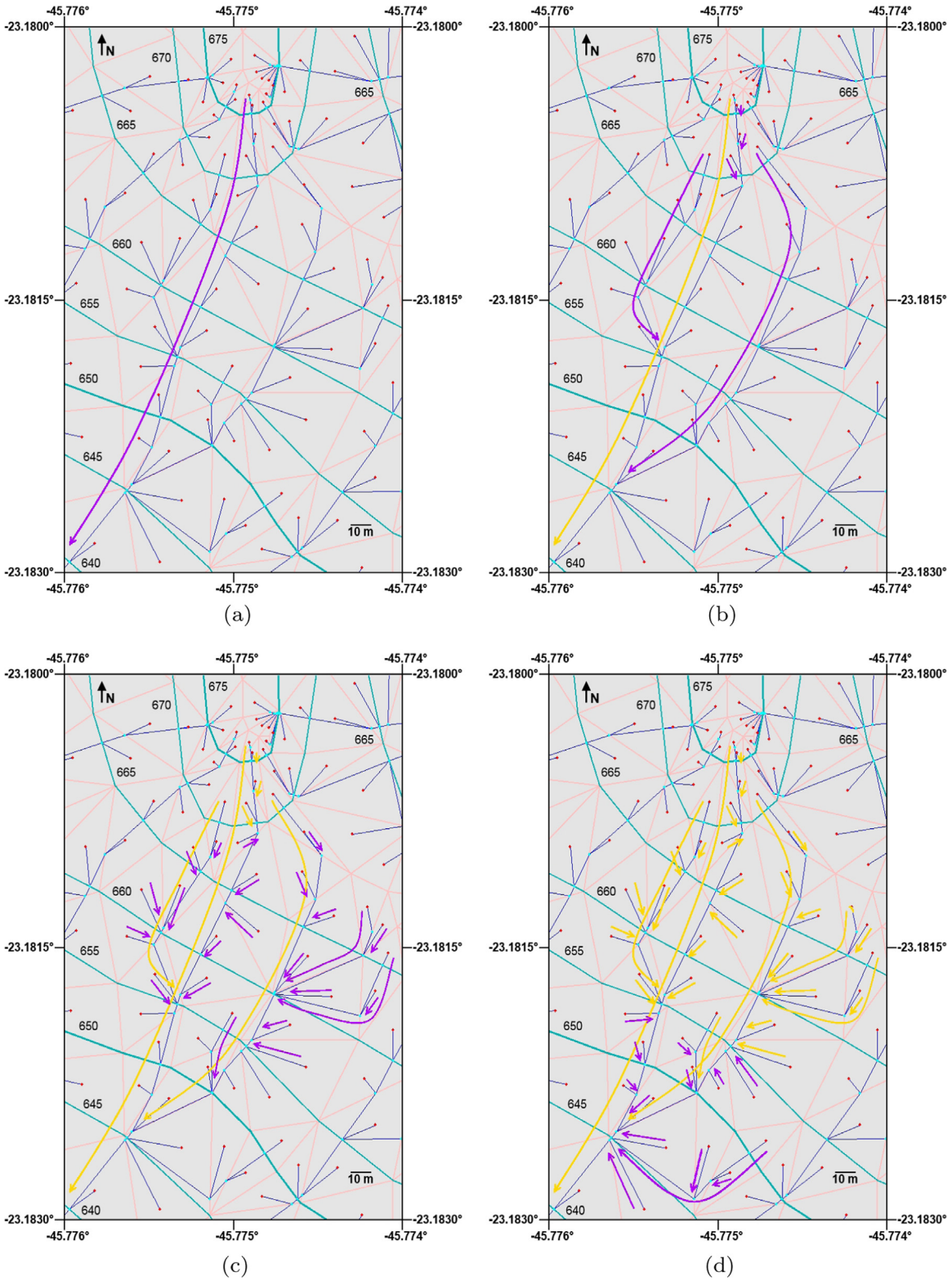

Fig. 6. Connection of drainage paths – (a) First drainage path (purple) starts at a higher triangle centroid. (b) Subsequent paths are connected to the first path (orange). (c) New paths are connected to previous paths. (d) Paths from lower centroids are connected to the existing paths. (For interpretation of the references to color in this figure caption, the reader is referred to the web version of this paper.)

Different schemes were devised for pit removal from TINs. A lifting approach (Silveira and van Oostrum, 2007; Silveira, 2009) works by lifting the pit elevation to the lowest elevation of its neighboring points, then including the lowest neighbor as part of a new pit consisting of more than one point, and this lifting process is repeated until a lower elevation point is reached. This procedure is also known as flooding technique with the drawback that all the points that form the pit define a flat area, so it introduces another inconsistency into the terrain model.

Another distinct approach removes pits by lowering the elevation of points that form paths between the pit and points of

lower elevation, where each path has associated a cost or significance value to be minimized in order to reduce the changes in the terrain model (Silveira and van Oostrum, 2007; Silveira, 2009). This technique is similar to a common solution used for removing pits from regular grids known as carving process (Soille et al., 2003).

In this work, the procedure developed for pit removal is based on the lowering approach, but considering paths without costs. The paths of points include either only critical points (the points used for removing flat areas), if the pit is a critical point, or both critical and contour line points, if the pit is a contour line point, in order to minimize the changes in the elevation of the original points (Freitas, 2014). The elevation of each point included in a path is linearly interpolated between the initial and final points, as performed for flat areas.

3. Extraction of drainage networks and watersheds

3.1. Hydrological modeling

To a large extent, the main use of drainage networks and watersheds is commonly related to hydrological models developed to address several problems in water resources management.

For instance, the DHSVM (Distributed Hydrology Soil Vegetation Model) (Wigmosta et al., 2002) has been used to study interactions between climate and hydrology, potential impacts of climate change on water resources, forest management activities on watershed processes, and runoff estimation with transport of water, sediments, chemicals, and nutrients. Similarly, the MGB-IPH distributed hydrological model (Collischonn et al., 2007) focuses on the rainfall-runoff analysis in large-scale basins.

The CHILD (Channel-Hillslope Integrated Landscape Development) model (Tucker et al., 2001a,b) simulates the evolution of a topographic surface and its subjacent stratigraphy under a set of driving erosion and sedimentation processes with initial and boundary conditions for investigating problems in catchment geomorphology. The TIN-based Real-Time Integrated Basin Simulator (tRIBS) (Vivoni et al., 2004) is a physically-based and distributed hydrological model that emphasizes the dynamic relationship between a partially saturated vadose zone and the land surface response to the continuous storm and interstorm cycle due to groundwater flow and evapotranspiration demand.

The first two models consider the spatial information in a regular grid, the third one works on either a regular grid or a TIN, and the last one on TINs.

3.2. Flow directions

Several techniques were developed for the extraction of hydrological results directly from TINs. One approach determines how water is routed on the TIN surface by considering two different conditions between triangles, namely In-In-Out and In-Out-Out cases (Silfer et al., 1987), depending on how flows enter and exit each triangle side according to the directions given by the vectors normal to the triangles. However, as the flows are defined from only two particular cases, this determines a restriction that hinders the generation of more natural water-flow patterns.

A method described by Jones et al. (1990) presents many important concepts with the flow directions given by the gradient vectors calculated from the plane of each triangle in order to define paths of steepest descent. This method includes the fundamental techniques used in this work as the basis for the generation of drainage paths, so that the main details of its formulation and procedures are presented in the next subsection.

Slingsby (2003) proposes a method for drainage extraction from a TIN where the edges of the triangulation are changed, thus relaxing the Delaunay criterion in order to make the flows fully connected. Overland flows indicate which edges must be changed to provide a continuous drainage network, although these overland flows are not part of it. The resulting drainage paths include many parallel flows, therefore the paths are not hydrologically consistent.

Another approach by Tsirogiannis (2011) defines trickle paths traced in a sequence of edges and vertices, called an EV-sequence, considered as a set of terrain features determined from the paths of steepest descent (Jones et al., 1990). Flows are not restricted to specific directions or limited only to follow through triangles edges, but it is not specified how drainage networks can be derived from the trickle paths.

A more recent work by Guodong et al. (2014) presents a method for the extraction of drainage networks and watersheds

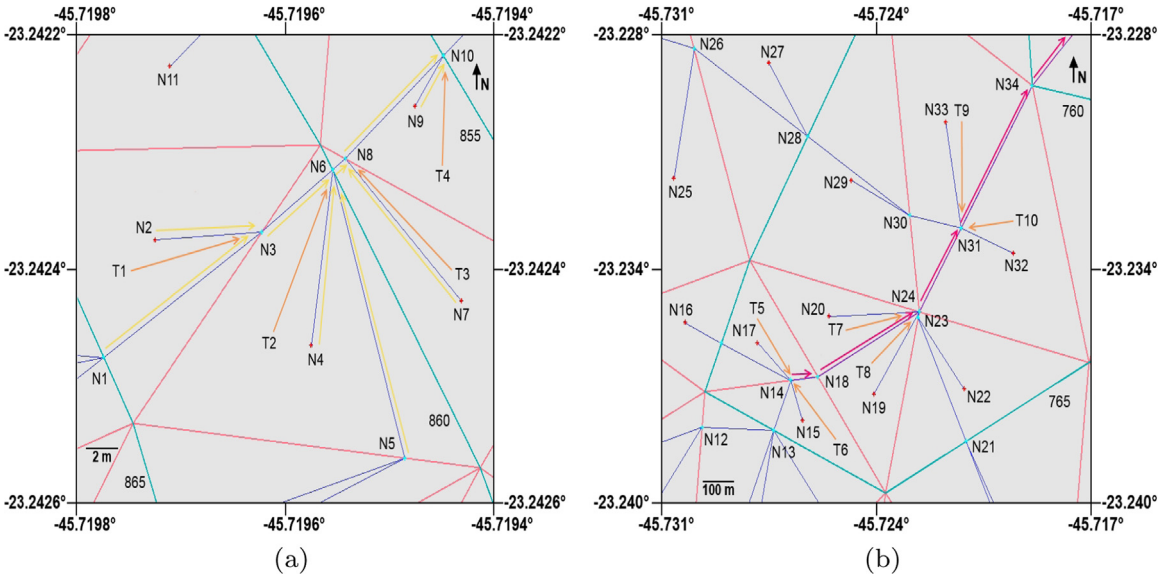

Fig. 7. Different cases of contributing areas from triangles (orange arrows) - (a) Contributing areas from triangles *T*1, *T*2, *T*3 and *T*4 crossed by flow segments (overland flows). (b) Contributing areas from triangles *T*7 and *T*8 adjacent by channel edges (channel flows). (For interpretation of the references to color in this figure caption, the reader is referred to the web version of this paper.)

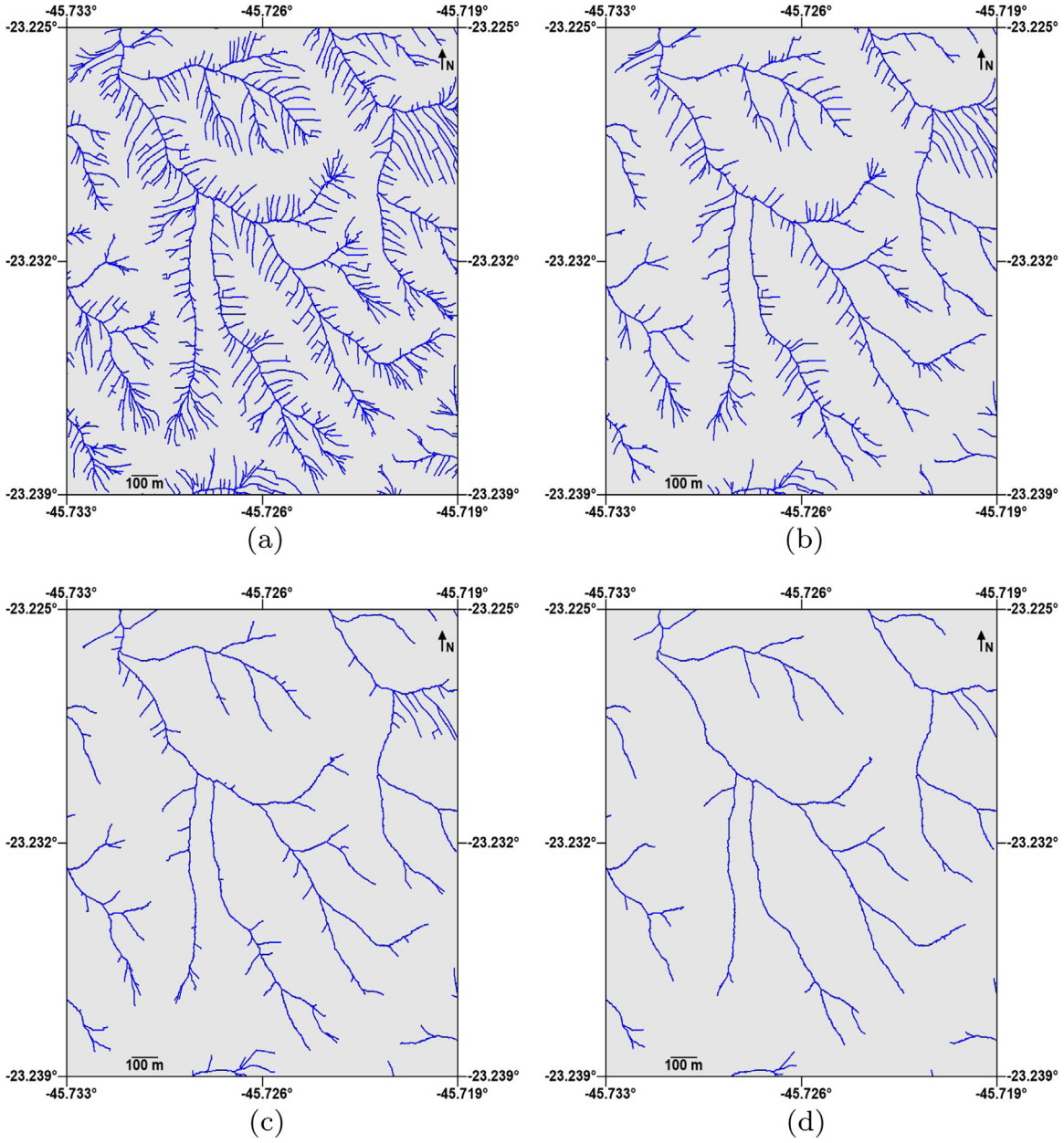

Fig. 8. Drainage networks generated from different threshold values T - (a) $T=1000$, (b) $T=2000$, (c) $T=4000$, and (d) $T=8000$.

from accumulated flows on the TIN. The method also defines flow directions from the gradient vectors, although it considers the flows only through triangles edges, either along channel edges or edges chosen from a particular condition that verifies the difference between two contributing areas in a triangle that are separated by the gradient vector. This approach constitutes a simplified model that changes flow directions, and thus inserts a restriction in the sequence of flows.

Despite the similarities of the aforementioned methods, no description is given on the use of drainage paths that strictly follow paths of steepest descent on the TIN for the generation of drainage networks from accumulated flows. This work describes how gradient vectors of triangles can form a proposed drainage graph structure that allows the calculation of accumulated flows for the extraction of drainage networks from arbitrary threshold values with the subsequent delineation of watersheds.

3.3. Drainage paths

TIN terrain models are continuous piecewise linear functions obtained from a set of points that represents the terrain surface. Usually, the flow of water in a terrain model is a purely geometrical problem that does not consider aspects such as soil type and land cover (Tsirogiannis, 2011). However, this exclusively geometrical representation defines good-quality approximations of terrain surfaces and their associated drainage patterns.

As previously mentioned, this work considers drainage paths based on the flow directions given by gradient vectors calculated from the TIN (Jones et al., 1990). Each triangle with vertices $v_1 = (x_1, y_1, z_1)$, $v_2 = (x_2, y_2, z_2)$ and $v_3 = (x_3, y_3, z_3)$ defines a linear plane (Eq. (3)) with coefficients A, B, C and D determined from the coordinates of each point (Eqs. (4)–(7)).

$$Ax + By + Cz + D = 0 \tag{3}$$

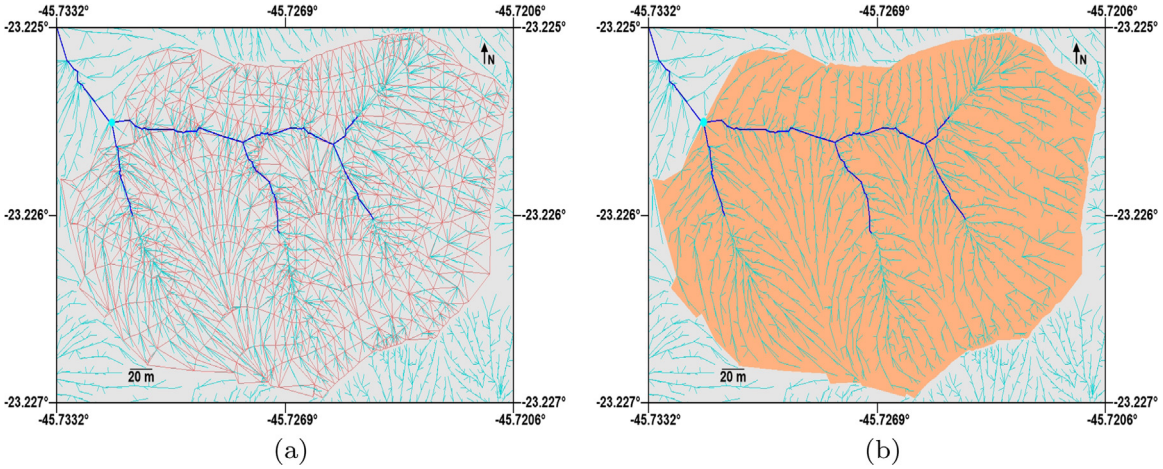

Fig. 9. Watershed delineated from the flow segments of the drainage graph – (a) Triangles crossed by the flow segments. (b) Watershed delineated from the flow segments. (For interpretation of the references to color in this figure, the reader is referred to the web version of this paper.)

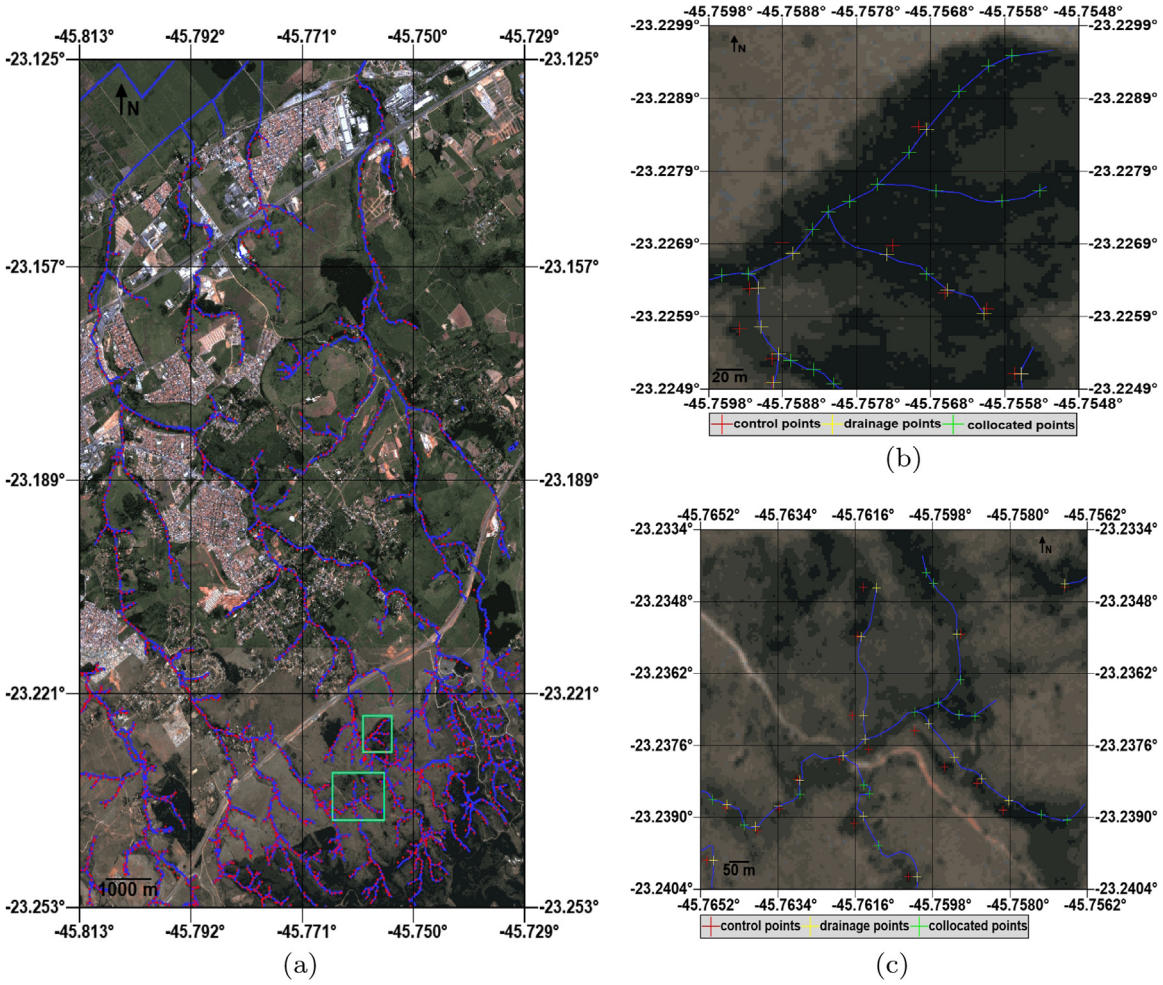

Fig. 10. Area of study – (a) Reference drainage network (blue) together with control points (red). (b) Region depicted by the upper rectangle in (a). (c) Region depicted by the lower rectangle in (a). (For interpretation of the references to color in this figure caption, the reader is referred to the web version of this paper.)

$$A = y_1(z_2 - z_3) + y_2(z_3 - z_1) + y_3(z_1 - z_2) \quad (4)$$

$$B = z_1(x_2 - x_3) + z_2(x_3 - x_1) + z_3(x_1 - x_2) \quad (5)$$

$$C = x_1(y_2 - y_3) + x_2(y_3 - y_1) + x_3(y_1 - y_2) \quad (6)$$

$$D = -Ax_1 - By_1 - Cz_1 \quad (7)$$

From Eq. (3), writing the elevation z as a function of the coordinates x and y (Eq. (8)), and then calculating the negative gradient of this function (Eq. (9)), the direction of steepest descent is given by the vector components $\frac{A}{C}$ and $\frac{B}{C}$ that represent the x and y

variations in the flow direction to be followed from a point in a triangle, respectively:

$$z = f(x, y) = -\left(\frac{A}{C}x + \frac{B}{C}y + \frac{D}{C}\right) \tag{8}$$

$$-\nabla f = \frac{A}{C}\vec{i} + \frac{B}{C}\vec{j} \tag{9}$$

The drainage paths are traced from the gradient vectors of the triangles by following either from a vertex or from an intersection with an edge (Jones et al., 1990). In this work, drainage paths start at the centroid of the triangles ordered from highest to lowest with elevations considered as priority values associated to each triangle (Freitas et al., 2013). Moreover, when a drainage path reaches a triangle where another path is already defined, then the current path is just connected to the existing path at the outflow of the triangle.

Steps of this procedure are illustrated in Fig. 6 that includes triangles centroids (red), and intersections between triangles edges and drainage paths (cyan). The first drainage path is traced from a higher centroid, then other drainage paths are traced from lower centroids in subsequent steps, and connected to the outflows previously defined. At the end, this procedure generates a drainage structure that represents the flow directions on the TIN (Freitas, 2014).

It is noteworthy that drainage paths strictly following paths of steepest descent on the TIN, either across the triangles or along the edges, define better approximations of the water flows in contrast to simplified models that only consider flows along the edges, thus restricted to just part of the TIN surface, and affecting the quality of the flows (Tsirogiannis, 2011).

3.4. Drainage graph

The drainage structure obtained from the drainage paths is referred to as drainage graph (Freitas, 2014), which allows the calculation of accumulated flows for the generation of drainage networks by threshold values. The drainage graph comprises nodes and edges defined from the drainage paths with nodes represented by triangles centroids, intersections between gradient vectors and triangles edges, and also vertices of channel edges, whereas edges by flow segments across the triangles (overland flows) and along the edges (channel flows).

Relevant properties of the drainage graph for the calculation of accumulated flows are: (a) it defines a tree structure as a directed acyclic graph, not presenting cycles between the nodes; (b) flow directions are unique for any node, by the standard flow model in digital terrain analysis (Tsirogiannis, 2011).

Each flow segment between two nodes defines a flow direction that promptly indicates the source (upstream) and destination (downstream) of the water flow accumulated from node to node added with the contributing areas of the triangles in two different cases: (a) the area of the triangle crossed by a flow segment (yellow arrows in Fig. 7(a)); (b) the sum of the areas of two triangles adjacent by a channel edge that contains a flow segment (purple arrows in Fig. 7(b)). Additionally, even though a node N may present upstream nodes with different flow segments crossing the same triangle, the contributing area of the triangle is accumulated only once in the node N.

It is important to mention that if the downstream node of a flow segment is located along a channel edge, and the upstream node is located at another edge (overland flow), then the contributing area accumulated from the downstream node to the lowest vertex of the channel edge is equal to zero, in order to avoid the contributing areas to be accumulated twice from node to node in a sequence of flows along channel edges. This particular case is depicted in Fig. 7(b) where the contributing areas accumulated from node $N14$ to $N18$, and from node $N31$ to $N34$ are zero, i.e., the accumulated flows from the nodes $N14$ and $N31$ are not added with any contributing areas.

Fundamentally, the accumulated flows are calculated from a *topological sort* (Cormen et al., 2001) of the nodes by starting at all the nodes of in-degree zero, i.e., nodes without upstream nodes. Whenever all the upstream nodes of a node p are already processed, then the flow of p is accumulated in its downstream node added with the contributing areas defined by its flow segment, so that this procedure continues until all the nodes are processed.

3.5. Drainage networks and watersheds

Drainage networks are key components in hydrological models and in resource management plans (O'Callaghan and Mark, 1984) providing significant information on water resources, possible flood areas, erosion, and other natural processes (Agarwal et al., 1996). In essence, drainage networks represent the main courses

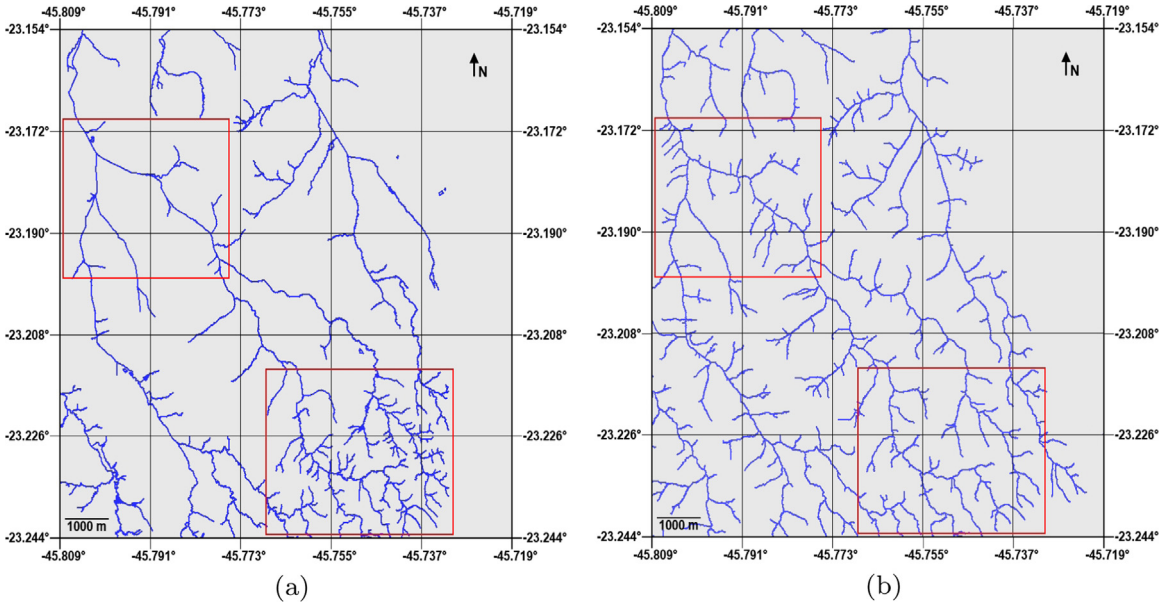

Fig. 11. Drainage networks – (a) Reference drainage network. (b) TIN drainage network.

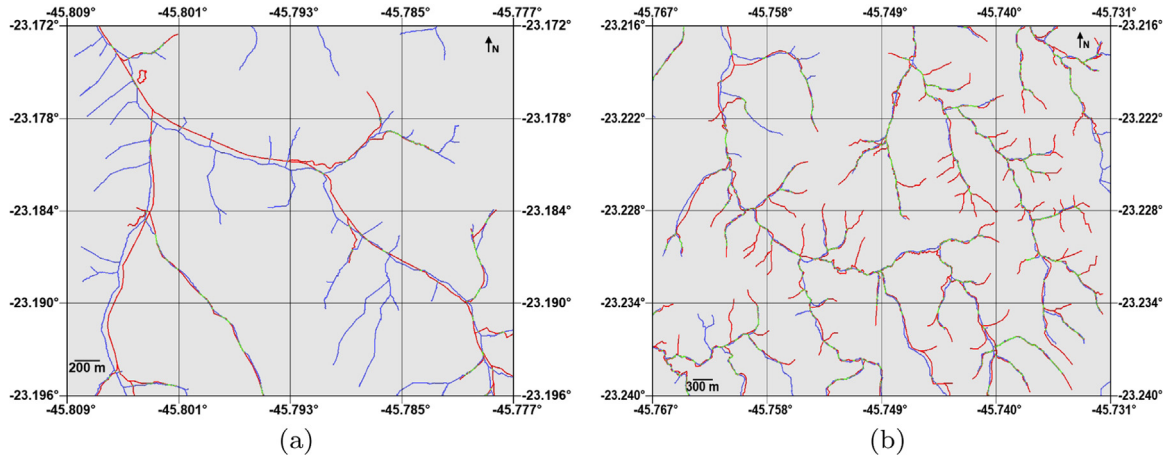

Fig. 12. Overlap between the reference (red) and the TIN (blue) drainage networks with collocated points (green). (For interpretation of the references to color in this figure caption, the reader is referred to the web version of this paper.)

of water on a terrain surface, and can be used for the delineation of watersheds that play an important role in hydrological studies with a wide variety of applications (Zhang et al., 1990).

In this work, drainage networks are generated from the drainage graph by including all the flow segments that contain nodes with accumulated flows equal to or greater than a given threshold. An example of drainage networks generated from different threshold values is illustrated in Fig. 8, indicating that the lower the threshold value, the higher the number of flow segments included in the drainage network.

As important as drainage networks, watersheds form natural units in hydrology because the amount of water that flows out of a watershed can be measured and used in hydrological computations. More precisely, a watershed is defined as the region that contributes water to a particular point on the terrain surface, considered the watershed's outlet point.

In a TIN, a watershed is delineated from any initial point located on the drainage network by recursively following the flow segments connected to each upstream node reachable from the initial point along the drainage paths, then including all the triangles traversed in the process as part of the watershed. Since this work considers flow segments strictly following paths of steepest descent, the watershed delineation in this case represents a more realistic approximation (Guercio and Soccodato, 1996; Tsirogiannis, 2011; Yu et al., 1996) in contrast to one that only considers channel edges (Jones et al., 1990).

Fig. 9 exhibits all the flow segments (light blue) of a given region that contribute to the flows accumulated in the nodes of a drainage network (dark blue) defined from an arbitrary threshold value of 8000 m^2. Fig. 9(a) includes the triangles crossed by the flow segments that delineate the watershed illustrated in Fig. 9 (b) from the initial point at the left (cyan).

Besides the delineation of a single watershed, it is also possible to subdivide a given watershed into several subwatersheds, where this subdivision depends on the drainage segments present in the drainage network. The points where the drainage network presents branches define different drainage segments, and each drainage segment is associated to a particular subwatershed.

4. Results

The input dataset used in this work for the generation of the TIN is composed of 202,137 points that define contour lines in intervals of 5 m and sampled points irregularly distributed over a geographic region of 753.6 km^2 ranging from −45.813° to −45.712° in longitude, and from −23.253° to −23.122° in latitude, in São José dos Campos (Brazil). All the points are located at an average distance of 17.03 m between each other. Fig. 10 (a) exhibits the area of study with a RapidEye image of 5 m resolution from 2011 (BlackBridge, 2008).

The hydrological results obtained from the TIN are qualitatively and quantitatively compared to a reference drainage network (blue lines in Fig. 10(a)) manually produced by specialists from an analysis of contour maps and available in the 'Living City' database (Cidade, 2003).

The reference drainage network presents an average accuracy of 9.29 m calculated from 1800 points in the high-resolution image that represent the first 90% of 2000 control points (red dots in Fig. 10(a)) arranged in a non-decreasing sequence according to the distance between two corresponding points that are located on the reference drainage network and on the water courses present in the high-resolution image. Figs. 10(b) and (c) show the regions depicted by the upper and lower rectangles in Fig. 10(a), respectively, illustrating control points, drainage points, and also collocated points where the location of the first two is the same.

Fig. 11 exhibits the reference and the TIN drainage networks for an extent of the area of study. The main courses of water are present in both drainage networks, indicating that high-quality and real-world consistent drainage networks can be automatically generated from TIN terrain models. In this example, the TIN drainage network was generated from a threshold of 40,000 m^2.

Differences in the number and length of the drainage segments are expected because the reference drainage network is a result from a subjective analysis of contour maps whereas the TIN drainage network is generated from a fixed threshold value. Therefore it is unlikely that all the courses of water in each drainage network can match exactly.

The red rectangles in Fig. 11 highlight some of the differences, where the region indicated below presents a higher number of drainage segments in the reference drainage network when compared to the TIN drainage network, whereas the opposite occurs in the region highlighted above. These regions are illustrated with more details in Figs. 12(a) and (b) for the upper and lower rectangles, respectively, showing the reference and the TIN drainage networks overlapped together with collocated points, visually indicating the main similarities and differences between the drainage segments of each drainage network.

In order to quantify the differences between the reference and the TIN drainage networks, Table 1 presents values of the length of the drainage segments (Agrawal et al., 2006; McCoy, 1970) as well

Table 1
Measures from drainage segments of the reference and the TIN drainage networks for different threshold values.

Threshold (m^2)	Segments																			
28,000	Number	1			2			3–5–7			8–11			9			12–15–17			13–19	
	Reference length (m)	43.3			424.8			600			365.1			166.9			382.3			259.9	
	TIN length (m)	44.2			387.3			621.3			356.3			133.3			317.9			266.3	
	TIN-reference length (m)	0.9			−37.5			21.3			−8.8			−33.6			−64.4			6.4	
	Area between segments (m^2)	38.3			2873.9			2318.1			1524.1			851.8			983.6			1580.3	
	Average distance (m)	0.4			3.7			1.9			2.1			3.2			1.5			3	
12,000	Number	1	2	3	4	5	6	7	8	9	10	11	12	13	14	15	16	17	18	19	20	21
	Reference length (m)	43.3	424.8	382.4	177	142.7	200.8	74.9	87.7	166.9	103.7	277.4	108.3	68.5	96	118.9	73	155.1	131.2	191.4	100.3	139.9
	TIN length (m)	44.2	455.9	382.5	144.8	149.5	121.3	92.6	97.2	133.3	101.1	275	122	70.4	28	125.6	38.7	90.1	68.2	201	93.5	115.5
	TIN-reference length (m)	0.9	31.1	0.1	−32.2	6.8	−79.5	17.7	9.5	−33.6	−2.6	−2.4	13.7	1.9	−68	6.7	−34.3	−65	−63	9.6	−6.8	−24.4
	Area between segments (m^2)	38.3	2945.2	1426.1	628.8	490.5	916.4	401.5	430.3	851.8	686.7	1093.8	345.3	199.9	77	300.6	155.4	389.4	160.9	1380.4	203.9	715.4
	Average distance (m)	0.4	3.2	1.9	2.2	1.6	3.8	2.2	2.2	3.2	3.4	2	1.4	1.4	1.4	1.2	2	2.2	1.2	3.4	1.1	3.1

as the area and the average distance between corresponding drainage segments (Collischonn et al., 2010), the latter calculated as the area divided by twice the length of the TIN drainage segment, thus representing an average distance in both directions from the segment. The values in Table 1 are related to Figs. 13 (a) and (b) with drainage networks generated from threshold values of 28,000 m^2 and 12,000 m^2, respectively.

The results in Table 1 indicate that for the region illustrated in Fig. 13, the drainage networks derived from the TIN present small differences with relation to the reference drainage network. In the first case, the TIN drainage network generated from a threshold of 28,000 m^2 has as minimum and maximum absolute length differences the values 0.9 m and 64.4 m with the average around 24.7 m. The minimum and maximum average distances between drainage segments are 0.4 m and 3.7 m around 2.3 m when considering the distances of all the segments.

In the second case, the TIN drainage network generated from a threshold of 12,000 m^2 presents absolute length differences ranging from 0.1 m to 79.5 m with the average around 24.3 m, and the average distances range from 0.4 m to 3.8 m around 2.1 m. These results exemplify how different threshold values produce drainage networks from the TIN with segments that may represent few or many of the real drainage patterns of the terrain without significant deviation and loss of quality.

The TIN results are also compared to drainage networks, watersheds and subwatersheds obtained from a regular grid processed with the TerraHidro software (TerraHidro, 2008) that is developed at the Image Processing Division (DPI) of the National Institute for Space Research (INPE).

The TerraHidro software is a distributed hydrological modeling system that ensures a better drainage extraction regarding the topographical aspects (Abreu et al., 2012; Rosim et al., 2013). The software removes flat areas with a carving process that creates a downward path from the border of the flat area until reaching the center, thus avoiding the generation of parallel drainage lines. It also removes pits by linearly re-interpolating the elevation values of specific points selected after performing a Priority-First Search (PFS) algorithm (Jones, 2002), in order to find a path of grid points between the pit and a nearby point of lower elevation by considering for each visited point the elevation difference as a priority value, so that the points are stored in a priority queue, and the point of smallest difference is selected.

In this work, the regular grid processed with the TerraHidro software was interpolated in 5 m cell resolution from the same input dataset used for the TIN with a weighted mean by quadrant and elevation method available in the Spring software (Camara et al., 1996). Regarding the comparison between the TIN and the regular grid results, Fig. 14 illustrates a region with part of the drainage networks obtained from each structure by considering the threshold value of 40,000 m^2. This example also includes the entire watersheds and the subwatersheds of each drainage segment, both delineated from initial points located on the drainage networks.

The drainage networks present approximate patterns, indicating that hydrological results derived from either a TIN or a regular grid reveal similarities between each other. Moreover, the watersheds and subwatersheds are also similar in size and shape, although local differences occur due to the distinct flow directions defined from each structure. For this reason, the areas around some regions (red circles) do not properly agree as one structure contains paths to the drainage segments with more flows whereas the other fewer flows.

Many factors can contribute to the occurrence of the differences between the hydrological results derived from each terrain model, such as the interpolation method used to generate the regular grid when it is not readily available, the procedures

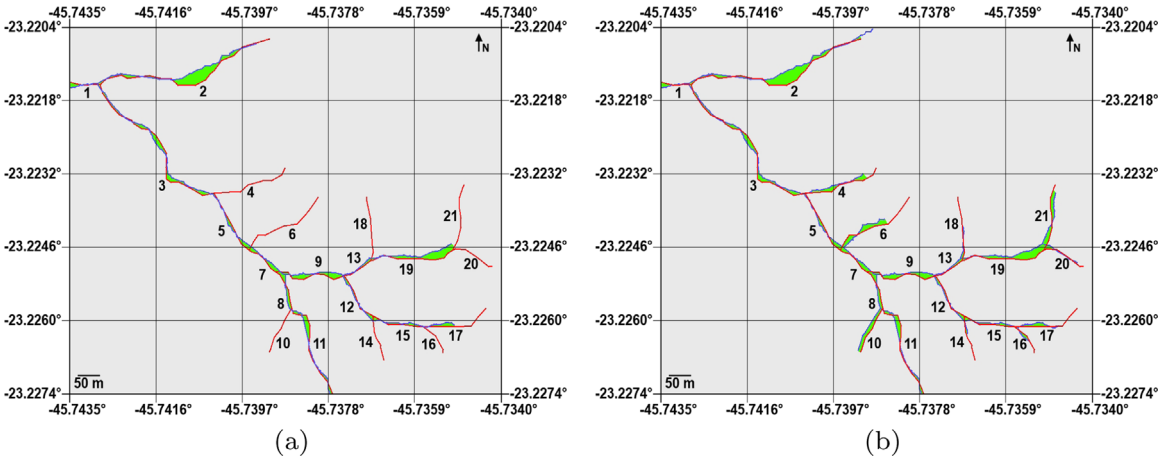

Fig. 13. TIN (blue) and reference (red) drainage networks with drainage segments numbered from 1 to 21, and the area between the segments (green) for thresholds of 28,000 m^2 (a) and 12,000 m^2 (b). (For interpretation of the references to color in this figure caption, the reader is referred to the web version of this paper.)

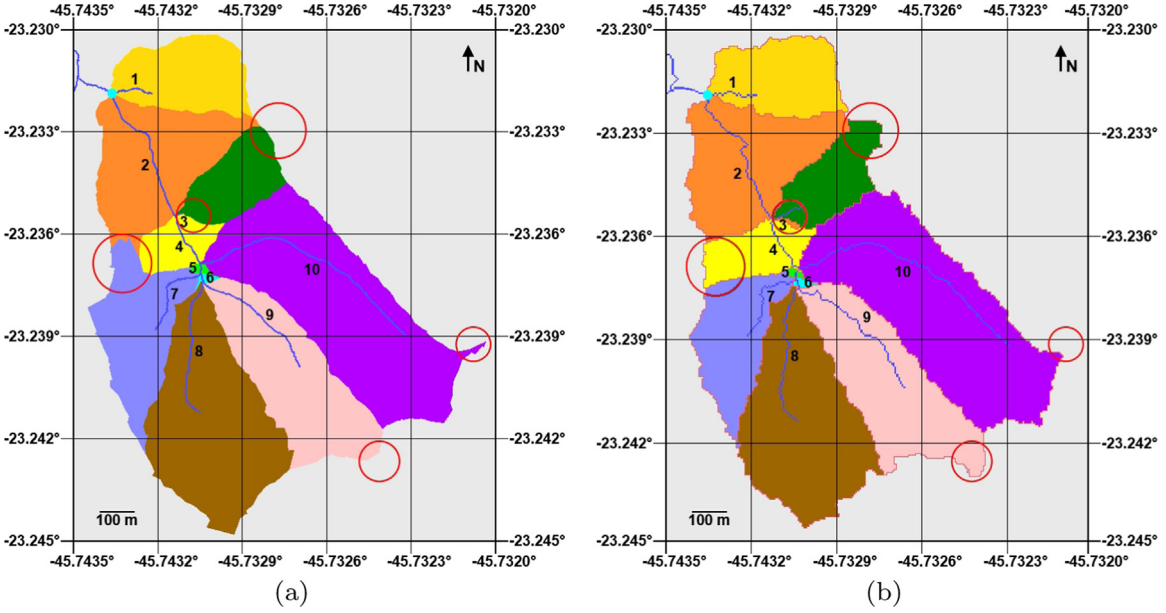

Fig. 14. Drainage networks, watersheds and subwatersheds delineated from initial points (cyan) for the TIN (left) and for the regular grid (right) with differences between subwatersheds indicated in some areas (red circles). (For interpretation of the references to color in this figure caption, the reader is referred to the web version of this paper.)

performed to remove inconsistencies of flat areas and pits, and also how the flow directions are defined from point to point.

A quantitative comparison between the TIN and the regular grid results for the region illustrated in Fig. 14 is presented in Table 2, which includes the length of the drainage segments, the area and the average distance between them. Additionally, Table 2 also includes the area and the perimeter of the watersheds and subwatersheds together with the differences between these measures.

The absolute length differences between corresponding drainage segments present minimum and maximum values equal to 1 m and 86.6 m, respectively, with the average around 44.6 m. The average distances between segments range from 0.5 m to 2 m around 1.3 m. These values indicate similar results derived from each structure with respect to the drainage networks. In addition, TIN segments are mostly shorter because these segments follow smoother paths.

However, the minimum and maximum absolute differences between the areas of the subwatersheds are 78 m^2 and 14,555 m^2, in this order, with an average of 4448.8m^2, and the perimeter absolute differences range from 30 m to 723 m around 382.6 m. These differences indicate that many flows defined from each terrain model follow distinct directions, thus aggregating different contribution areas, and changing the delineation. Despite of it, the percentage difference between the areas of the watersheds is small and approximately within 1%.

In order to illustrate how sensitive the drainage networks are if a different threshold value is considered, Fig. 15 exhibits the TIN and the regular grid drainage networks generated from a threshold of 25,000 m^2 for the same region of Fig. 14. In this case, the regular grid drainage network contains a drainage segment that is not present in the TIN drainage network, thus producing 3 new subwatersheds (indicated by the red circle).

For a detailed view of the data obtained by processing the TIN, Table 3 presents the output information for different number of input points, including the number of intersections between contour lines and triangles edges, and the number of flat triangles, both on the original TIN, as well as the number of triangles and pits on the final TIN, and also the number of nodes in the drainage graph.

Additionally, computational times are also an important aspect related to the algorithms developed in this work that perform

Table 2
Measures from drainage segments, watersheds and subwatersheds of the regular grid and the TIN drainage networks for the region in Fig. 14.

Number		1	2	3	4	5	6	7	8	9	10		
Segments	Regular grid length (m)	171.1	474.1	98.6	178.1	29.1	29.1	285.9	457.5	480.8	790		
	TIN length (m)	119.4	415.9	24.7	159.8	30.1	23.5	244.9	413.9	394.2	723.9		
	TIN-grid length (m)	−51.7	−58.2	−73.9	−18.3	1	−5.6	−41	−43.6	−86.6	−66.1		
	Area between segments (m^2)	264.2	1694.8	84.9	250.9	116.4	23.1	661.5	949.9	1296.4	1303.5		
	Average distance (m)	1.1	2	1.7	0.8	1.9	0.5	1.4	1.1	1.6	0.9		
Subwatersheds	Regular grid area (m^2)	68,700	111,400	49,125	37,650	975	1275	70,250	155,075	124,300	215,250	Watersheds	834,000
	TIN area (m^2)	68,431	113,500	47,141	26,400	1513	1197	84,805	164,769	121,977	213,553		843,286
	TIN-grid area (m^2)	−269	2100	−1984	−11, 250	538	−78	14,555	9694	−2323	−1697		9286
	Regular grid perimeter (m)	1440	2240	1340	1180	190	200	1740	2340	2360	3090		4664
	TIN perimeter (m)	1142	1649	914	692	220	160	1619	1866	1725	2367		4332
	TIN-grid perimeter (m)	298	591	426	488	30	40	121	474	635	723		332

Table 3
Output information.

Points	Intersections	Flat triangles	Triangles	Pits	Drainage graph nodes
51,145	2398	24,804	15,2554	209	307,447
100,928	7469	32,421	26,7600	179	539,189
150,605	10,446	47,623	39,7810	164	802,175
202,137	15,861	54,644	514,578	12	1,037,775

linear-time DFS and BFS procedures. All the algorithms were implemented in C++, compiled in a 64-bit machine, and executed on a PC with Intel Core i7 2.93 GHz CPU and 8 GB of memory. The TIN computational times are shown in Table 4 together with the computational times obtained from regular grids of different resolutions and number of cells (rows by columns) processed with the TerraHidro software.

The TIN execution times include the following procedures: constrained Delaunay triangulation; removal of flat areas and pits; re-triangulation with critical points; calculation of the gradient vector of each triangle; generation of the drainage paths; definition of the drainage graph; and calculation of accumulated flows. The regular grid execution times include the removal of flat areas and pits, the generation of flow directions, and the calculation of accumulated flows.

One consideration about this comparison is that the TIN computational times depend mainly on the number of triangles because most of the procedures are performed on the TIN, with the only exception of the accumulated flows that are calculated from the nodes of the drainage graph. The regular grid computational times depend predominantly on the number of grid cells. From Table 4, by comparing the execution times from closer numbers of triangles and grid cells such as, for instance, 267,600 triangles and 273,452 grid cells or even 514,578 triangles and 485,450 grid cells, both presenting similar resolutions, the results indicate that the algorithms developed for the TIN are likely to be more computationally efficient.

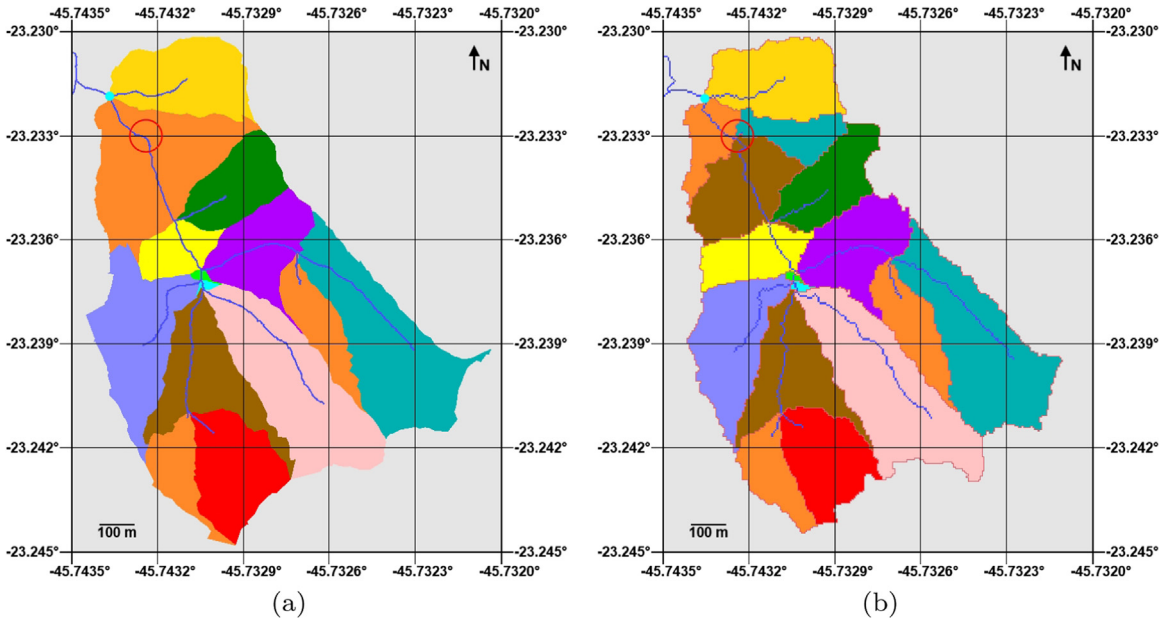

Fig. 15. Drainage networks, watersheds and subwatersheds delineated from initial points (cyan) for the TIN (left) and for the regular grid (right) for a threshold value of 25,000 m^2. (For interpretation of the references to color in this figure caption, the reader is referred to the web version of this paper.)

Table 4
TIN and regular grid computational times.

TIN				Regular grid		
Points	Triangles (average area)	Drainage graph nodes	Execution time (s)	Cells (R × C)	Resolution (m)	Execution time (s)
51,145	152,554 (608.15 m^2)	307,447	2.34	273,452 (548 × 499)	20	75.8 (1 min 15 s)
100,928	267,600 (346.11 m^2)	539,189	3.87	485,450 (730 × 665)	15	177.12 (2 min 57 s)
150,605	397,810 (255.30 m^2)	802,175	5.77	1,091,715 (1095 × 997)	10	308.24 (5 min 8 s)
202,137	514,578 (207.09 m^2)	1,037,775	9.02	4,369,050 (2190 × 1995)	5	1848.86 (30 min 48 s)

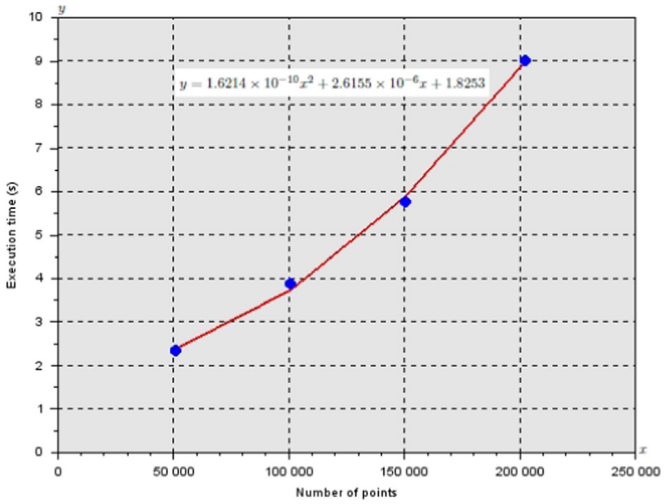

Fig. 16. Execution times for a different number of input points with fitting curve (red) adjusted to the data. (For interpretation of the references to color in this figure caption, the reader is referred to the web version of this paper.)

The execution times as a function of the number of input points can be visualized in Fig. 16 as a dispersion plot (blue) together with a fitting curve given by a quadratic regression function (red). From the equation of the quadratic polynomial curve, the fitting adjusts to the data with a R^2 coefficient equals to 0.9985.[1]

5. Conclusions

This work considered the extraction of drainage networks and watersheds from terrain models represented by TINs. Inconsistencies in the TIN, such as flat areas and pits, were removed with specific procedures in order to improve its quality for the generation of more exact hydrological results.

More importantly, a proposed drainage graph structure defined from drainage paths that strictly follow paths of steepest descent allowed to derive drainage networks from accumulated flows on the TIN that were qualitatively and quantitatively consistent with the main courses of water present in a real-world reference drainage network, presenting small differences and thus reinforcing that the TIN is an attractive alternative to other terrain models, specially for hydrological applications. Moreover, all the algorithms developed for the TIN presented low computational times.

Additionally, qualitative and quantitative comparisons between hydrological results generated from the TIN and from the regular grid showed approximate patterns with drainage networks mostly agreeing on the quantity and lengths of the drainage segments as well as watersheds and subwatersheds presenting regions considerably similar in size and shape, although differences in some of the subwatersheds occurred due to the distinct flow directions defined from each terrain model.

All the results indicate that the procedures presented in this work can be used in hydrological models for the generation of essential and useful drainage patterns to decision-making systems that support studies and researches of natural phenomena and environmental issues based on hydrological processes.

As future work, one intends to include the procedures described in this work as hydrology-specific functionalities in the TerraHidro computational system with the Terralib library (Camara et al., 2000) developed at DPI/INPE, a library of GIS classes and functions for spatial databases available as an open source project, thus providing the end user with a broad and rich set of tools for hydrological applications, not limited to only one type of terrain model. In addition, the procedures developed to remove flat areas and pits can be modified to allow the user to properly identify the regions of flat landscapes or water bodies that must not be modified in order to not present flows and drainage paths. A sensitivity analysis of the hydrological results when using contour lines in different elevation intervals can be also considered.

Acknowledgments

This research was financially supported by CAPES (Coordenação de Aperfeiçoamento de Pessoal de Nível Superior) from the Brazilian Education Ministry (MEC), and conducted as part of a master's thesis submitted by the first author to the graduate course in Applied Computing of the National Institute for Space Research (INPE) (code 33010013002P1) under the advisement of the other authors. The elevation data and reference drainage network were supplied by the Geoprocessing Service of the Urban Planning Department of the city of São José dos Campos (Brazil).

[1] If the R^2 coefficient of a regression curve derived from a sampled data equals to 1.0, then the curve perfectly fits the data (Kirk, 2008).

Appendix

See Algorithms 1 and 2.Algorithm 1

Algorithm CP = RemoveFlatAreas(T)

Input: A set T of triangles in the plane

Output: A set CP of critical points with elevation values interpolated

```
1  Initialize set CT with all nct corner triangles of T (flat triangles first, then not flat);
2  Initialize set CP with all critical points in T;
3  Mark all critical points in CP as not visited and not interpolated;
4  for i ← 1 to nct do
5      Set DiffElevPointFound = false;
6      Initialize empty queue BT of branching triangles;
7      Initialize empty set CPPATH of critical points;
8      Initialize empty set FIRSTPATH of critical points;
9      for j ← 1 to 3 do
10         if edge e_j of CT_i is critical and point cp_j is not visited or interpolated then
11             Mark cp_j as visited;
12             Insert point of CT_i opposite to e_j as initial point into CPPATH;
13             Insert critical point cp_j into CPPATH;
14             // traverse triangles from adjacent triangle adj_j
15             DefinePathOfTriangles(adj_j);
16             if DiffElevPointFound = true and elevation of initial point of CPPATH is
                equal to the flat area then
17                 Interpolate elevation of critical points in CPPATH;
18             else
19                 if elevations of initial and final points of FIRSTPATH are equal to the
                    flat area then
20                     Define elevation of middle point in FIRSTPATH as the elevation of
                        the flat area incremented by the contour lines interval (hilltop);
21                 else
22                     Define elevation of middle point in FIRSTPATH as the mean
                        between the elevation of the flat area and the initial point (saddle);
23                 end
24                 Interpolate elevations from initial to middle points in FIRSTPATH;
25                 Interpolate elevations from middle to final points in FIRSTPATH;
26             end
27         end
28         while BT is not empty do
29             Set DiffElevPointFound = false;
30             Remove branching triangle BRT from BT;
31             Initialize empty set CPPATH of critical points;
32             Insert interpolated critical point of BRT as initial point into CPPATH;
33             DefinePathOfTriangles(BRT);
34             Interpolate elevation of critical points in CPPATH;
35         end
36     end
37 end
38 Return: CP;
```

Algorithm 2

Function CP = DefinePathOfTriangles(t)

Input: A triangle t in the plane

Output: A set CP of critical points with elevation values to be interpolated

```
1  if t is a corner triangle and contains point p with elevation different from the flat area or
     from the initial point in CPPATH then
2      Set DiffElevPointFound = true;
3      Insert p into CPPATH;
4      Return: CPPATH;
5  end
6  for i ← 1 to 3 do
7      if DiffElevPointFound = true then
8          Return: CPPATH;
9      end
10     if t contains 3 critical points not interpolated and t is not in BT then
11         Insert t into queue BT of branching triangles;
12     end
13     if edge e_i of t is critical and point cp_i is not visited or interpolated then
14         Mark cp_i as visited;
15         Insert critical point cp_i into CPPATH;
16         if FIRSTPATH is empty and adjacent triangle adj_i is a corner triangle then
17             Define FIRSTPATH = CPPATH;
18             Insert point of adj_i opposite to e_i into FIRSTPATH;
19         end
20         // traverse triangles from adjacent triangle adj_i
21         DefinePathOfTriangles(adj_i);
22         if DiffElevPointFound = false then
23             Remove last point from CPPATH;
24             Mark cp_i as not visited;
25         end
26     end
27 end
28 Return: CPPATH;
```

References

Abreu, E.S., Rosim, S., Renno, C.D., Oliveira, J.R.F., Jardim, A.C., Ortiz, J.O., Dutra, L.V., 2012. Terrahidro—a distributed hydrological system to delimit large basins. In: International Geoscience and Remote Sensing Symposium—IGARSS. IEEE, Munich, Germany, pp. 546–549. URL: ⟨http://ieeexplore.ieee.org/xpl/articleDetails.jsp?arnumber=6351535&tag=1⟩, http://dx.doi.org/10.1109/IGARSS.2012.6351535.

Agarwal, P., de Berg, M., Bose, P., Dobrindt, K., van Kreveld, M.J., Overmars, M.H., de Groot, M., Roos, T., Snoeyink, J., Yu, S., 1996. The complexity of rivers in triangulated terrains. In: Fiala, F., Kranakis, E., Sack, J.R. (Eds.), The Eighth Canadian Conference on Computational Geometry—CCCG, Carleton University Press, pp. 325–330. URL: ⟨http://www.cccg.ca/proceedings/1996/⟩.

Agrawal, R., Ahmad, N., Jayprasad, P., Mahtab, A., Kumar, J.A.V., Pathan, S.K., 2006. Comparative evaluation of various algorithms for drainage extraction using CARTOSAT-1 stereo data. Agric. Hydrol. Appl. Remote Sens. 6411, 1–11. http://dx.doi.org/10.1117/12.697907.

Barbalic, D., Omerbegovic, V., 1999. Correction of horizontal areas in TIN terrain modeling—algorithm. In: Proceedings of the 19th Annual ESRI International User Conference. ESRI, San Diego, CA, USA. URL: ⟨http://proceedings.esri.com/library/userconf/proc99/proceed/papers/pap924/p924.htm⟩.

Berg, M.d., Cheong, O., Kreveld, M.v., Overmars, M., 2008. Computational Geometry: Algorithms and Applications, 3rd ed. Springer-Verlag, Santa Clara, CA, USAhttp://dx.doi.org/10.1007/978-3-540-77974-2, URL: ⟨http://dl.acm.org/citation.cfm?id=1370949⟩ 386 pp..

BlackBridge, 2008. RapidEye—Satellite Imagery. URL: ⟨http://www.blackbridge.com/rapideye/index.html⟩.

Bowyer, A., 1981. Computing Dirichlet tessellations. Comput. J. 24, 162–166. http://dx.doi.org/10.1093/comjnl/24.2.162, URL: ⟨http://comjnl.oxfordjournals.org/content/24/2/162.abstract⟩.

Camara, G., Souza, R.C.M., Freitas, U.M., Garrido, J., 1996. SPRING: integrating remote sensing and GIS by object-oriented data modelling. Comput. Graph. 20, 395–403. http://dx.doi.org/10.1016/0097-8493(96)00008-8, URL: ⟨http://www.sciencedirect.com/science/article/pii/0097849396000088⟩.

Camara, G., Souza, R.C.M., Pedrosa, B.M., Vinhas, L., Monteiro, A.M.V., Paiva, J.A., Carvalho, M.T., Gattass, M., 2000. TerraLib: technology in support of GIS innovation. In: Proceedings of the II Brazilian Symposium on Geoinformatics—GeoInfo2000. INPE, UNICAMP-DCC and Tecgraf PUC-RIO, Sao Paulo, SP, Brazil, pp. 1–8. URL: ⟨http://www.geoinfo.info/geoinfo2000/papers/019.pdf⟩.

Chen, Z., Guevara, J.A., 1987. Systematic selection of very important points (VIP) from digital terrain model for constructing triangular irregular networks. In: Chrisman, N.R. (Ed.), The Eighth International Symposium on Computer-Assisted Cartography—Auto-Carto VIII, American Congress on Surveying and Mapping. American Society for Photogrammetry and Remote Sensing, Baltimore, MD, USA, pp. 50–56. URL: ⟨http://www.mapcontext.com/autocarto/proceedings/auto-carto-8/pdf/pages61-67.pdf⟩.

Cidade Viva, 2003. Banco de Dados 'Cidade Viva'. URL: ⟨http://www.sjc.sp.gov.br/secretarias/planejamento_urbano/geoprocessamento.aspx⟩ (in Portuguese).

Cignoni, P., Montani, C., Scopigno, R., 1998. DeWall: a fast divide and conquer Delaunay triangulation algorithm. Comput.-Aid. Des. 30, 333–341. http://dx.doi.org/10.1016/S0010-4485(97)00082-1, URL: ⟨http://www.sciencedirect.com/science/article/pii/S0010448597000821⟩.

Collischonn, W., Allasia, D., Silva, B.C., Tucci, C.E.M., 2007. The MGB-IPH model for large-scale rainfall-runoff modelling. Hydrol. Sci. J. 52, 878–895. http://dx.doi.org/10.1623/hysj.52.5.878, URL: ⟨http://www.tandfonline.com/doi/abs/10.1623/hysj.52.5.878#.VG3gAjTF-lc⟩.

Collischonn, W., Buarque, D.C., Paz, A.R., Mendes, C.A.B., Fan, F.M., 2010. Impact of pit removal methods on DEM derived drainage lines in flat regions. In: AWRA 2010 Spring Specialty Conference. American Water Resources Association, Orlando, FL, USA. URL: ⟨http://www.ct.ufpb.br/~adrianorpaz/artigos/Collischonn_et_al_AWRAconference_2010.pdf⟩.

Cormen, T.H., Stein, C., Rivest, R.L., Leiserson, C.E., 2001. Introduction to Algorithms, 2nd ed. McGraw-Hill Higher Education 976 pp..

Eastman, J.R., 2001. Idrisi32 Release 2—Guide to GIS and Image Processing. Clark Labs, Worcester, MA, USA, URL: ⟨http://gisak.vsb.cz/~pen63/DPZ_pro_geodety/Guide2.pdf⟩ 144 pp..

Fortune, S., 1987. A sweepline algorithm for Voronoi diagrams. Algorithmica 2, 153–174. http://dx.doi.org/10.1007/BF01840357, URL: ⟨http://link.springer.com/article/10.1007%2FBF01840357⟩.

Fowler, R.J., Little, J.J., 1979. Automatic extraction of irregular network digital terrain models. SIGGRAPH Comput. Graph. 13, 199–207. http://dx.doi.org/10.1145/965103.807444, URL: ⟨http://dl.acm.org/citation.cfm?id=807444⟩.

Freitas, H.R.A., 2014. Drainage Networks and Watersheds Delineation Derived from TIN-based Digital Elevation Models (Master's thesis). Instituto Nacional de Pesquisas Espaciais – INPE. URL: ⟨http://urlib.net/8JMKD3MGP3W/3HDPRRS⟩. 93 pp.

Freitas, H.R.A., Rosim, S., Oliveira, J.R.F., Freitas, C.C., 2013. Drainage paths derived from TIN-based digital elevation models. In: Proceedings of the XIV Brazilian Symposium on Geoinformatics—GeoInfo2013. CCST, INPE and UNICAMP-IC, Campos do Jordao, SP, Brazil, pp. 31–42. URL: ⟨http://www.geoinfo.info/proceedings_geoinfo2013.split/paper4.pdf⟩.

Guercio, R., Soccodato, F.M., 1996. GIS procedure for automatic extraction of geomorphological attributes from TIN-DTM. In: HydroGIS 96: Application of Geographic Information Systems in Hydrology and Water Resources Management. International Association of Hydrological Sciences (IAHS), Vienna, Austria, pp. 175–182. URL: ⟨http://hydrologie.org/redbooks/a235/iahs_235_0175.pdf⟩.

Guibas, L.J., Knuth, D.E., Sharir, M., 1992. Randomized incremental construction of Delaunay and Voronoi diagrams. Algorithmica 7, 381–413. http://dx.doi.org/10.1007/BF01758770, URL: ⟨http://link.springer.com/article/10.1007%2FBF01758770⟩.

Guodong, Q., Danyang, S., Zhanghua, L., 2014. A new algorithm to automatically extract the drainage networks and catchments based on triangulation irregular network digital elevation model. Journal of Shanghai Jiaotong University (Science) 19, 367–377. http://dx.doi.org/10.1007/s12204-014-1511-9, URL: ⟨http://link.springer.com/article/10.1007%2Fs12204-014-1511-9⟩.

Ivanov, V.Y., Vivoni, E.R., Bras, R.L., Entekhabi, D., 2004. Catchment hydrologic response with a fully distributed triangulated irregular network model. Water Resour. Res., 40. http://dx.doi.org/10.1029/2004WR003218, URL: ⟨http://onlinelibrary.wiley.com/doi/10.1029/2004WR003218/abstract⟩.

Jarvis, A., Reuter, H., Nelson, A., Guevara, E., 2008. Hole-filled SRTM for the globe version 4, available from the consortium for spatial information of the consultative group on international agricultural research (CGIAR-CSI) SRTM 90 m database. International Centre for Tropical Agriculture (CIAT) http://srtm.csi.cgiar.org.

Jenson, S.K., Domingue, J.O., 1988. Extracting topographic structure from digital elevation data for geographical information system analysis. Photogramm. Eng. Remote Sens. 54, 1593–1600, URL: ⟨http://edna.usgs.gov/edna/pubs/extractingtopographicstructure1.pdf⟩.

Jones, N.L., Wright, S.G., Maidment, D.R., 1990. Watershed delineation with triangle-based terrain models. J. Hydraul. Eng. – ASCE 116, 1232–1251. http://dx.doi.org/10.1061/(ASCE)0733-9429(1990)116:10(1232), URL: ⟨http://www.researchgate.net/publication/248378881_Watershed_Delineation_with_Triangle-Based_Terrain_Models⟩.

Jones, R., 2002. Algorithms for using a DEM for mapping catchment areas of stream sediment samples. Comput. Geosci. 28, 1051–1060. http://dx.doi.org/10.1016/S0098-3004(02)00022-5, URL: ⟨http://www.sciencedirect.com/science/article/pii/S0098300402000225⟩.

Kirk, R.E., 2008. Statistics—An Introduction, 5th ed. Thomson Wadsworth, URL: ⟨https://www.researchgate.net/publication/232905761_Kirk_R_E_2008_Statistics_An_introduction_5th_ed_Belmont_CA_Thompson_Wadsworth⟩.

McCoy, R.M., 1970. Automatic measurement of drainage networks. IEEE Trans. Geosci. Electron. 8, 178–182. http://dx.doi.org/10.1109/TGE.1970.271414, URL: ⟨http://ieeexplore.ieee.org/xpls/abs_all.jsp?arnumber=4043403&tag=1⟩.

O'Callaghan, J.F., Mark, D.M., 1984. The extraction of drainage networks from digital elevation data. Comput. Vis. Graph. Image Process. 28, 323–344. http://dx.doi.org/10.1016/S0734-189X(84)80011-0, URL: ⟨http://www.sciencedirect.com/science/article/pii/S0734189X84800110⟩.

O'Rourke, J., 1998. Computational Geometry in C, 2nd ed. University Press, New York, NY, USA 376 pp.

Petrie, G., Kennie, T.J.M., 1987. Terrain modelling in surveying and civil engineering. Comput.-Aid. Des. 19, 171–187. http://dx.doi.org/10.1016/0010-4485(87)90066-2, URL: ⟨http://dl.acm.org/citation.cfm?id=27486⟩.

Peucker, T.K., Douglas, D.H., 1975. Detection of surface-specific points by local parallel processing of discrete terrain elevation data. Comput. Graph. Image Process. 4, 375–387. http://dx.doi.org/10.1016/0146-664X(75)90005-2, URL: ⟨www.sciencedirect.com/science/article/pii/0146664X75900052⟩.

Rosim, S., Oliveira, J.R.F., Jardim, A.C., Namikawa, L.M., Renno, C.D., 2013. Terrahidro—a distributed hydrology modelling system with high quality drainage extraction. In: The Fifth International Conference on Advanced Geographic Information Systems, Applications, and Services—Geoprocessing 2013. International Academy, Research, and Industry Association—IARIA, Nice, France, pp. 161–167. URL: ⟨https://www.thinkmind.org/index.php?⟩.

Silfer, A.T., Kinn, G.J., Hassett, J.M., 1987. A geographic information system utilizing the triangulated irregular network as a basis for hydrologic modeling. In: The Eighth International Symposium on Computer-Assisted Cartography, pp. 129–136. URL: ⟨http://www.mapcontext.com/autocarto/proceedings/auto-carto-8/pdf/a-geographic-information-system-utilizing-the-triangulated-irregular-network.pdf⟩.

Silveira, R.I., 2009. Optimization of Polyhedral Terrains (Ph.D. thesis). Utrecht University. URL: ⟨http://www-ma2.upc.edu/rsilveira/pubs/PhDThesis.pdf⟩. 149 pp.

Silveira, R.I., van Oostrum, R., 2007. Flooding countries and destroying dams. In: Dehne, F.K.H.A., Sack, J.R., Zeh, N. (Eds.), The 10th International Workshop on Algorithms And Data Structures—WADS. Springer-Verlag, Halifax, Canada, pp. 227–238. URL: ⟨http://link.springer.com/chapter/10.1007%2F978-3-540-73951-7_21⟩, http://dx.doi.org/10.1007/978-3-540-73951-7_21.

Slingsby, A., 2003. An object-orientated approach to hydrological modelling using triangular irregular networks. In: The 11th Conference on GIScience and Research in UK 2003—GISRUK03, London, UK. URL: ⟨http://openaccess.city.ac.uk/568/⟩.

Soille, P., Vogt, J., Colombo, R., 2003. Carving and adaptive drainage enforcement of grid digital elevation models. Water Resour. Res. 39, 1366–1375. http://dx.doi.org/10.1029/2002WR001879.

TerraHidro, 2008. TerraHidro—Plataforma para modelagem hidrologica distribuida. URL: ⟨http://wiki.dpi.inpe.br/doku.php?id=terrahidro⟩ (in Portuguese).

Tsai, V.J.D., 1993. Delaunay triangulations in TIN creation: an overview and a linear-time algorithm. Int. J. Geogr. Inf. Syst. 7, 501–524. http://dx.doi.org/10.1080/02693799308901979, URL: ⟨http://www.tandfonline.com/doi/abs/10.1080/02693799308901979#.VG4O0jTF-lc⟩.

Tsirogiannis, C.P., 2011. Analysis of Flow and Visibility on Triangulated Terrains (Ph. D. thesis). Eindhoven University of Technology. URL: ⟨http://repository.tue.nl/717789⟩, http://dx.doi.org/10.6100/IR717789. 105 pp.

Tucker, G.E., Lancaster, S.T., Gasparini, N.M., Bras, R.L., 2001a. The channel-hillslope integrated landscape development model (CHILD). In: Harmon, R.S., Doe III, W. W. (Eds.), Landscape Erosion and Evolution Modeling. Springer, USA, pp. 349–388. http://dx.doi.org/10.1007/978-1-4615-0575-4, chapter 12.

Tucker, G.E., Lancaster, S.T., Gasparini, N.M., Bras, R.L., Rybarczyk, S.M., 2001b. An object-oriented framework for distribuited hydrologic and geomorphic modeling using triangulated irregular networks. Comput. Geosci. 27, 959–973. http://dx.doi.org/10.1016/S0098-3004(00)00134-5.

USGS, 2008. Global Land Survey Digital Elevation Model (GLSDEM). Global Land Cover Facility, University of Maryland. URL: ⟨http://glcf.umd.edu/data/glsdem/⟩.

Vivoni, E.R., Ivanov, V.Y., Bras, R.L., Entekhabi, D., 2004. Generation of triangulated irregular networks based on hydrological similarity. J. Hydrol. Eng. 9, 288–302. http://dx.doi.org/10.1061/(ASCE)1084-0699(2004)9:4(288).

Watson, D.F., 1981. Computing the *n*-dimensional Delaunay tessellation with application to Voronoi polytopes. Comput. J. 24, 167–172. http://dx.doi.org/10.1093/comjnl/24.2.167, URL: ⟨http://comjnl.oxfordjournals.org/content/24/2/167.abstract⟩.

Wigmosta, M.S., Nijssen, B., Storck, P., 2002. The distributed hydrology soil vegetation model. In: Mathematical Models of Small Watershed Hydrology and Applications. Water Resource Publications, Littleton, CO, USA, pp. 7–42 (Chapter 2). URL: ⟨http://ftp.hydro.washington.edu/pub/dhsvm/The-distributed-hydrology-soil-vegetation-model.pdf⟩.

Yu, S., Kreveld, M.V., Snoeyink, J., 1996. Drainage queries in TINs: from local to global and back again. In: The Seventh International Symposium on Spatial Data Handling. URL: ⟨http://www.oicrf.org/document.asp?ID=13630⟩.

Zhang, M.C., Campbell, J.B., Haralick, R.M., 1990. Automatic delineation of drainage basins within digital elevation data using the topographic primal sketch. Math. Geol. 22, 189–209. http://dx.doi.org/10.1007/BF00891823, URL: ⟨http://link.springer.com/article/10.1007%2FBF00891823⟩.

Zhu, Y.J., Yan, L., 2010. An improved algorithm of constrained Delaunay triangulation based on the diagonal exchange. In: The Second International Conference on Future Computer and Communication—ICFCC, vol. 1, pp. 827–830. URL: ⟨http://ieeexplore.ieee.org/xpls/abs_all.jsp?arnumber=5497312&tag=1⟩, http://dx.doi.org/10.1109/ICFCC.2010.5497312.